Gene circuit performance characterization and resource usage in a cell-free 'breadboard'

Dan Siegal-Gaskins[1,*], Zoltan A. Tuza[2,*], Jongmin Kim[1,*],Vincent Noireaux[3], and Richard M. Murray[1,4]

1. Division of Biology and Biological Engineering, California Institute of Technology, Pasadena, CA, USA
2. Faculty of Information Technology, Pazmany Peter Catholic University, Budapest, Hungary
3. School of Physics and Astronomy, University of Minnesota, Minneapolis, MN, USA
4. Department of Control and Dynamical Systems, California Institute of Technology, Pasadena, CA, USA

∗ These authors contributed equally to this work.

Supporting Information

Alternative performance metrics

For the purposes of characterization of a particular biocircuit testing environment, *in vitro* or *in vivo*, there are any number of performance metrics that may be used. We have chosen to use integrated mRNA and final protein concentration since they intuitively represent the total transcriptional and translational capacity of a system. Other metrics, such as the mRNA and protein production rates and end times, are complementary to those used in this work and may be particularly informative depending on the specific circuit or system requirement.

In Figs. S16 and S17 we show the maximum deGFP and MGapt production rates as a function of reporter concentration under different conditions. Using these measures, stark differences between simple one-stage gene expression and expression from the two-stage T7 cascade can be seen; for example, at low reporter concentrations, the maximum production rate of deGFP in the cascade is considerably larger than the one-stage rate, even when the strongest promoter is used. The cascade deGFP rates are also relatively flat with respect to reporter concentration. There is also a clear effect of NTPs on peak rates when a cascade is used versus simple expression. In the former case, additional NTPs provide for a significant increase in the maximum protein and mRNA production rates, whereas NTPs have little to no effect on maximum production rates for the Pr-deGFP-MGapt construct.

The deGFP production end time $t_{end,TL}$ is shown for all conditions in Fig. S18. $t_{end,TL}$ is between 330 and 350 minutes for simple expression in the 'linear' regime, but as high as ∼580 minutes in some of the conditions and concentrations tested. The end time is a particularly good measure of system capacity when extended performance is required.

Supplementary Figures

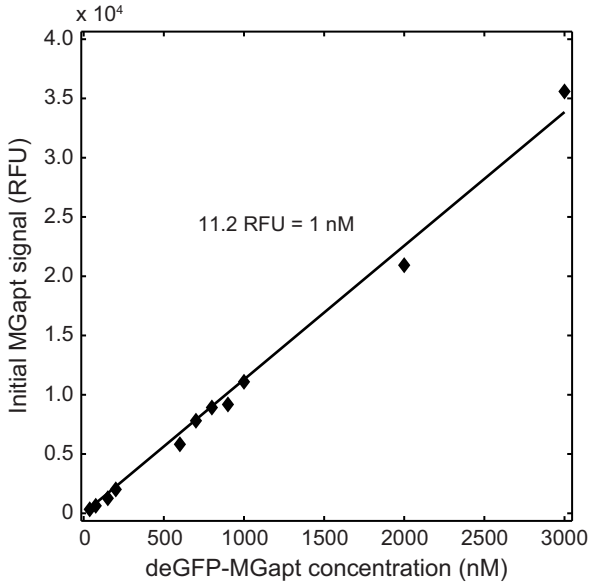

Figure S1: Calibration curve relating concentration of purified deGFP-MGapt transcript to initial MGapt fluorescence signal.

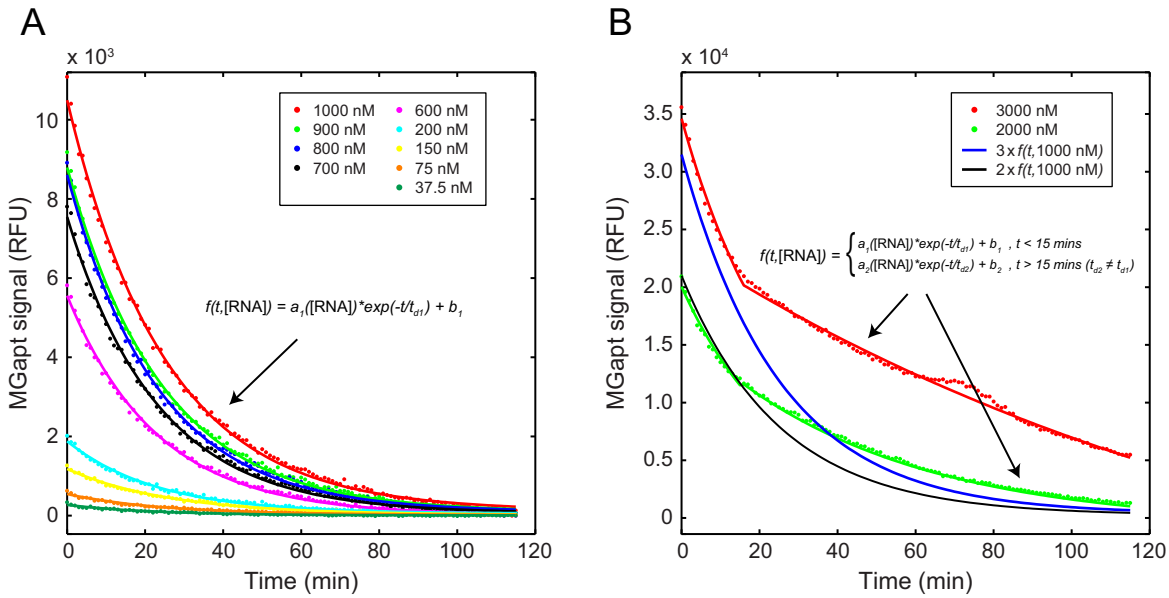

Figure S2: Decay of purified deGFP-MGapt transcripts in the cell-free breadboard. (A) Degradation is well-described by single exponential decay with 16–18 min half-lives for a wide range of concentrations. (B) At high concentrations, the decay curves follow those of the lower concentrations only to 15 min, after which the half-lives increase dramatically.

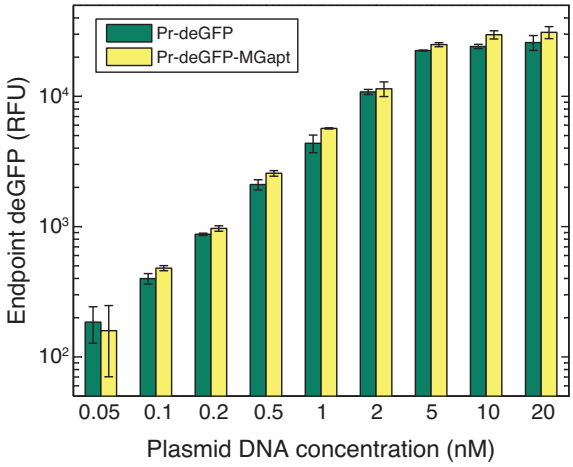

Figure S3: Comparison of total deGFP fluorescence produced by Pr-deGFP and Pr-deGFP-MGapt constructs. The incorporation of MGapt in the 3′ UTR downstream of deGFP leads to only a slight increase in the amount of protein produced relative to deGFP alone, a result we attribute to an increase in the stability of the fusion transcript conferred by the MGapt.

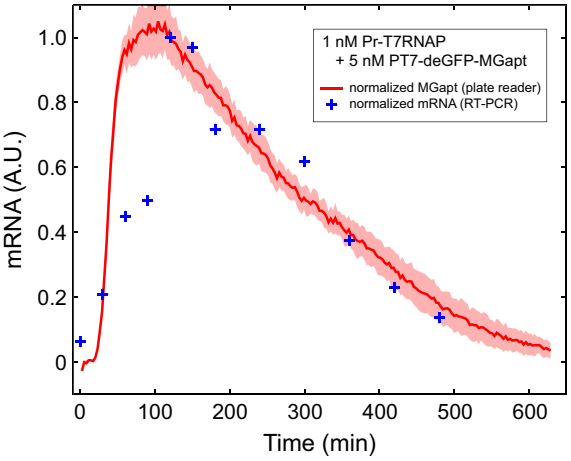

Figure S4: Comparison of normalized real-time PCR measurements and MGapt signal for the T7 RNAP cascade circuit (described in the section titled "Performance of a simple transcription–translation cascade") with 1 nM Pr-T7 RNAP and 5 nM PT7-deGFP-MGapt. Shaded region indicates standard error over replicates.

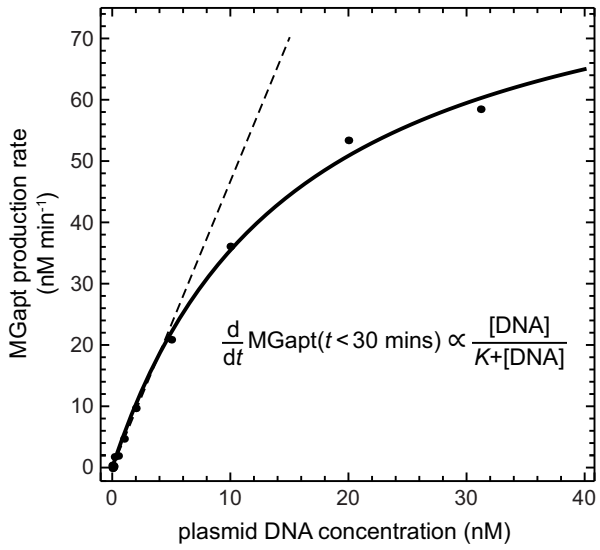

Figure S5: MGapt production at early times suggest transcriptional machinery is saturated as DNA concentration increases. Fits of MGapt production rates in the first 30 minutes of expression follow a Michaelis-Menten form with Michaelis constant K ∼15 nM.

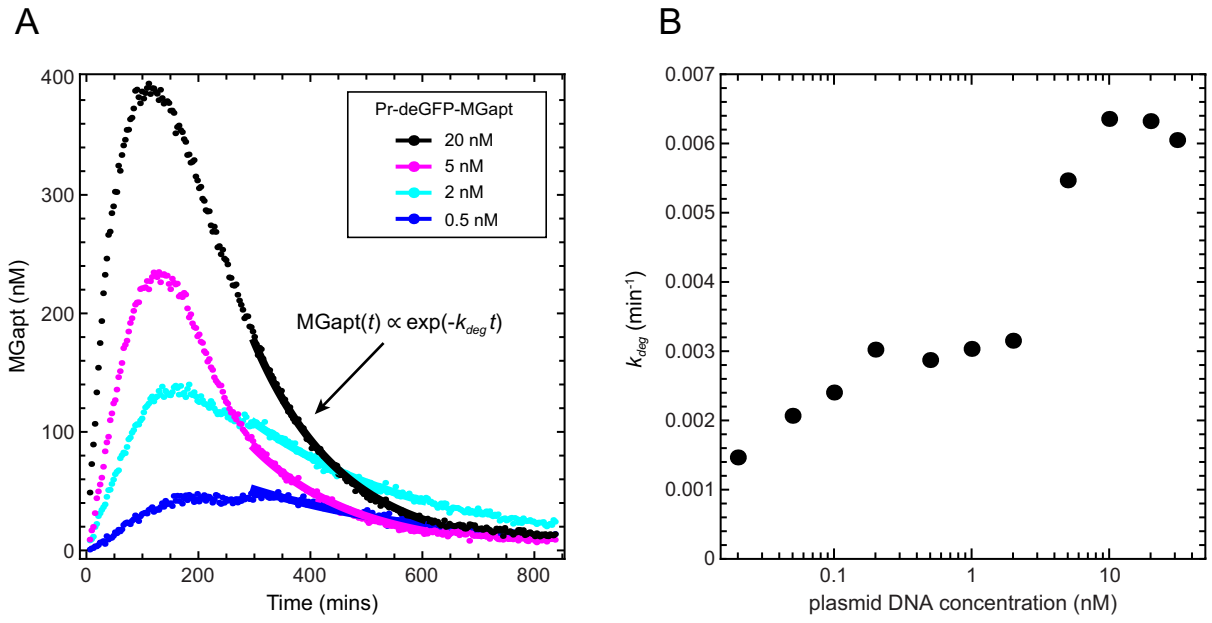

Figure S6: (A) MGapt expression curves are well-fit by a single exponential at late times. (B) Decay constants k_{deg} determined using a single exponential fit to data after 5 hours of expression. k_{deg} increases with increasing DNA concentration.

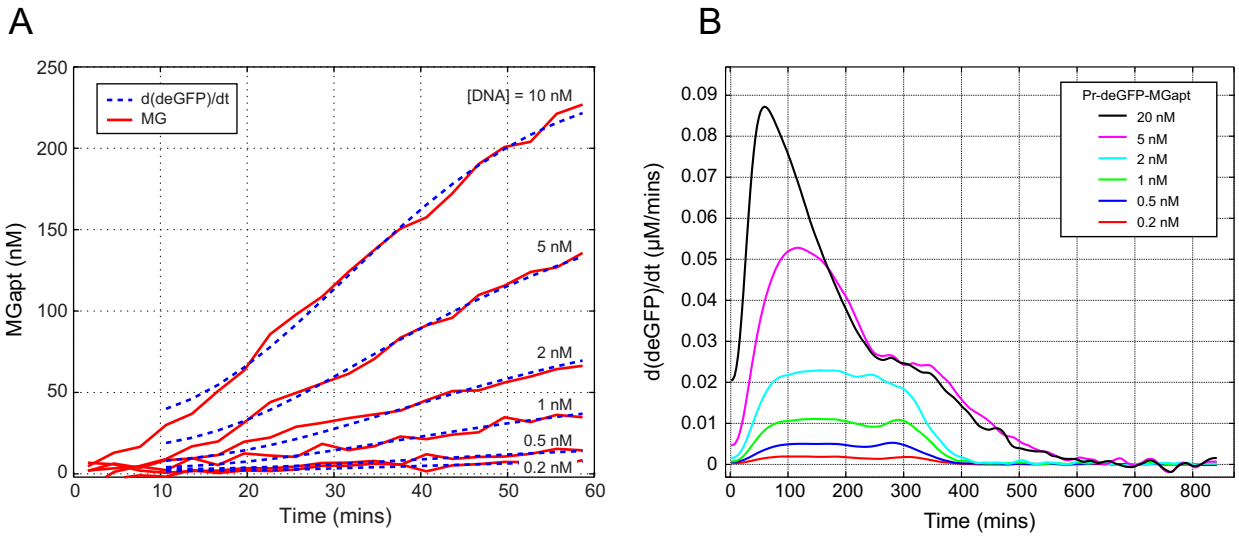

Figure S7: (A) The time derivative of the (spline fit) deGFP concentration is proportional to the MGapt concentration in the first hour of expression. (B) As the experiment goes on and the behavior of the system is no longer ideal, the shapes of the $\frac{\mathrm{d}}{\mathrm{d}t}\mathrm{deGFP}(t)$ deviate from $\mathrm{MGapt}(t)$ (although there remain significant qualitative similarities between them; cf. Fig. 1C.

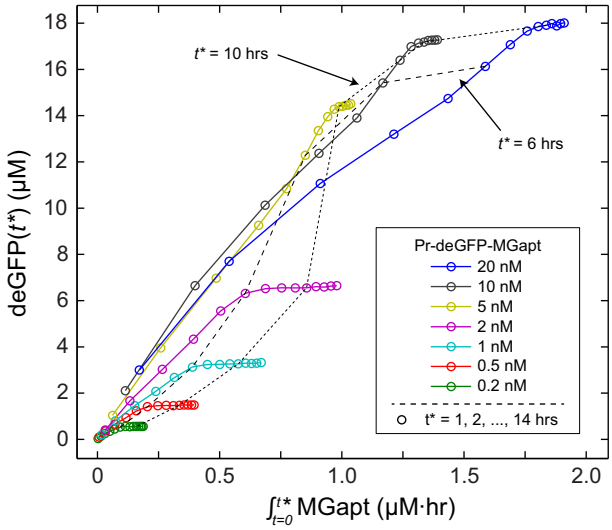

Figure S8: deGFP at various times t^* versus MGapt level integrated from time $t = 0$ to $t = t^*$ for a range of Pr-deGFP-MGapt concentrations, with $t^* = 1, 2, \ldots, 14$ hrs indicated with ○. Below the 'linear'–'saturation' regime transition concentration, $\int_{t=0}^{t*}\mathrm{MGapt}$ appears proportional to $\mathrm{deGFP}(t^*)$ until protein synthesis stops at $t^* \approx 340$ minutes, albeit with a proportionality constant that is different for different DNA template concentrations. Above the transition concentration, protein production stops later in the experiment and the $\int_{t=0}^{t*}\mathrm{MGapt}$ plateau is relatively short. Dashed lines showing $t^* = 6$ hrs and $t^* = 10$ hrs are shown for reference.

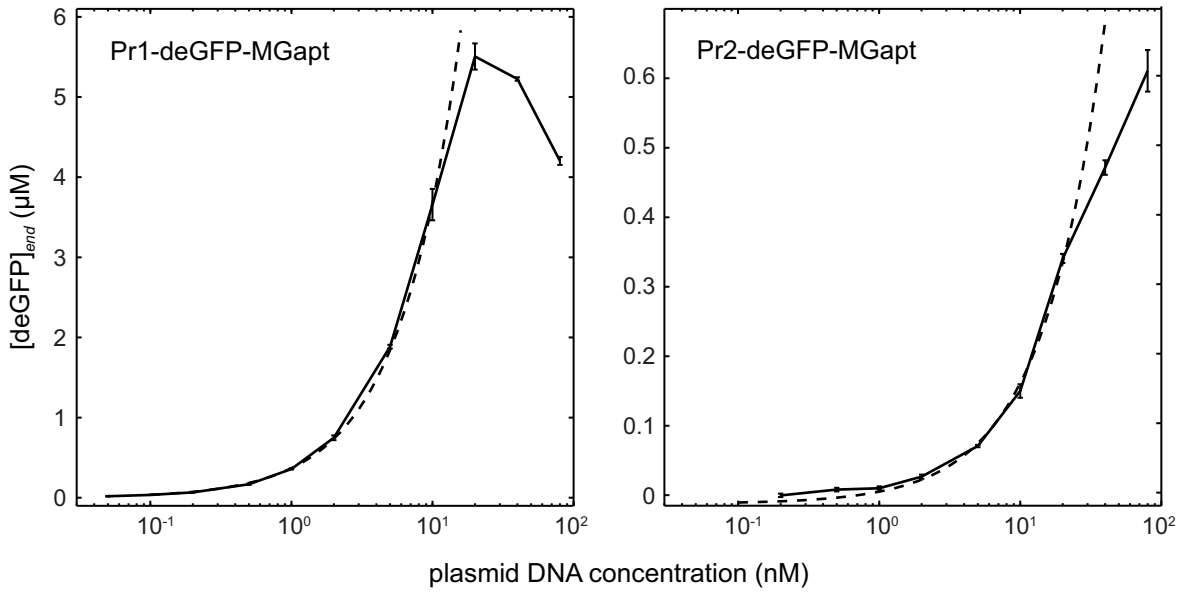

Figure S9: Endpoint deGFP versus plasmid concentration for weak promoters Pr1 (left) and Pr2 (right). Unlike the Pr promoter for which the linear regime ends at 2–5 nM DNA, for Pr1 and Pr2, the linear regime extends up to ∼10 nM and ∼20 nM, respectively. Dashed line shows a linear fit to the data.

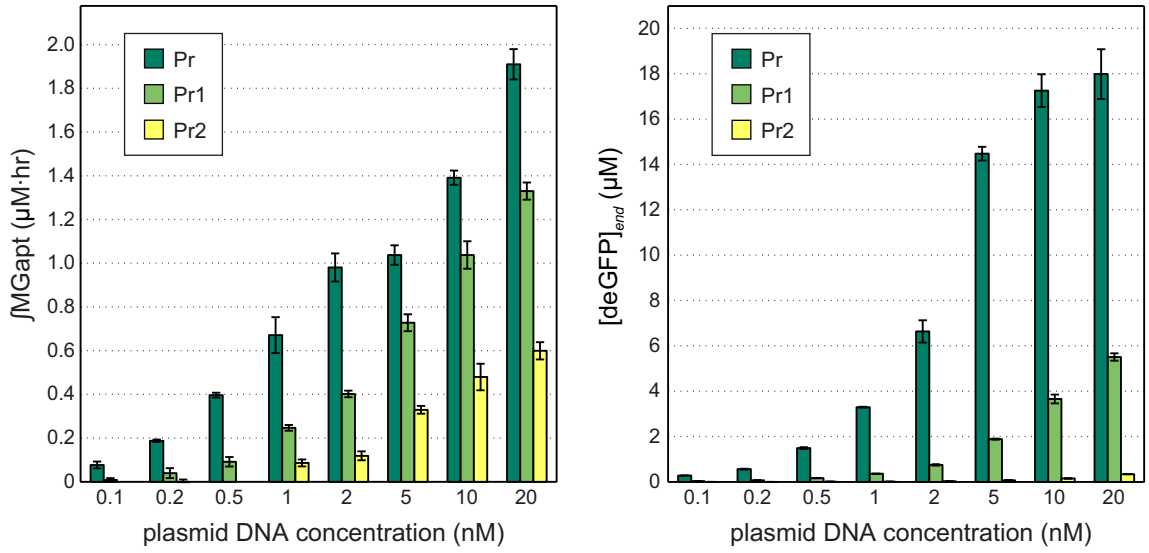

Figure S10: Comparison of integrated MGapt (left) and endpoint deGFP (right) for promoters Pr, Pr1, and Pr2.

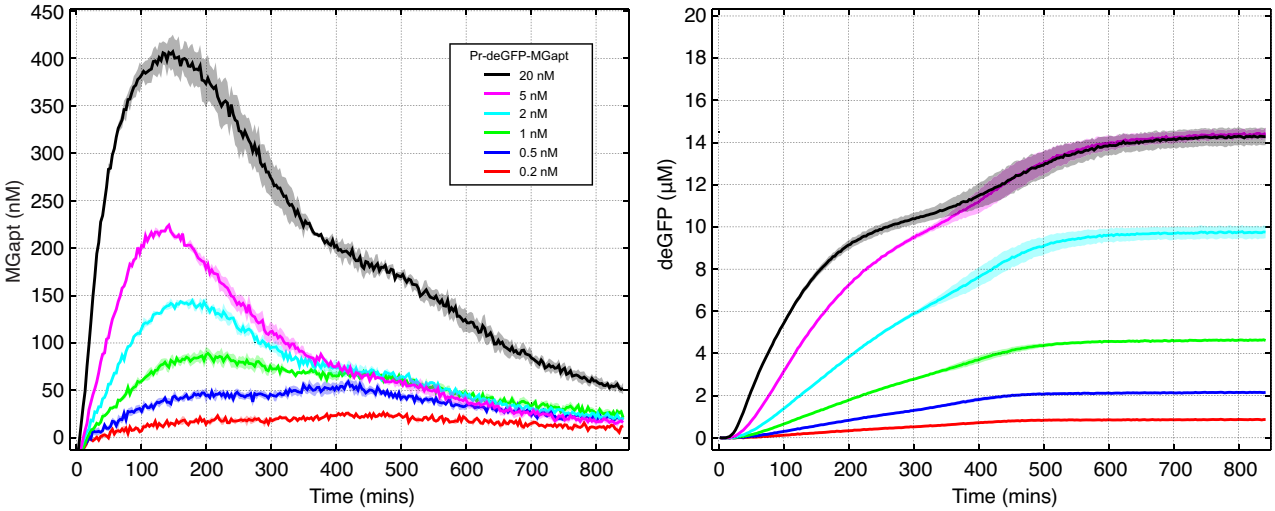

Figure S11: MGapt (left) and deGFP (right) expression kinetics when breadboard is supplemented with 1.25 mM of each of the four NTPs. Shaded regions indicate standard error over replicates.

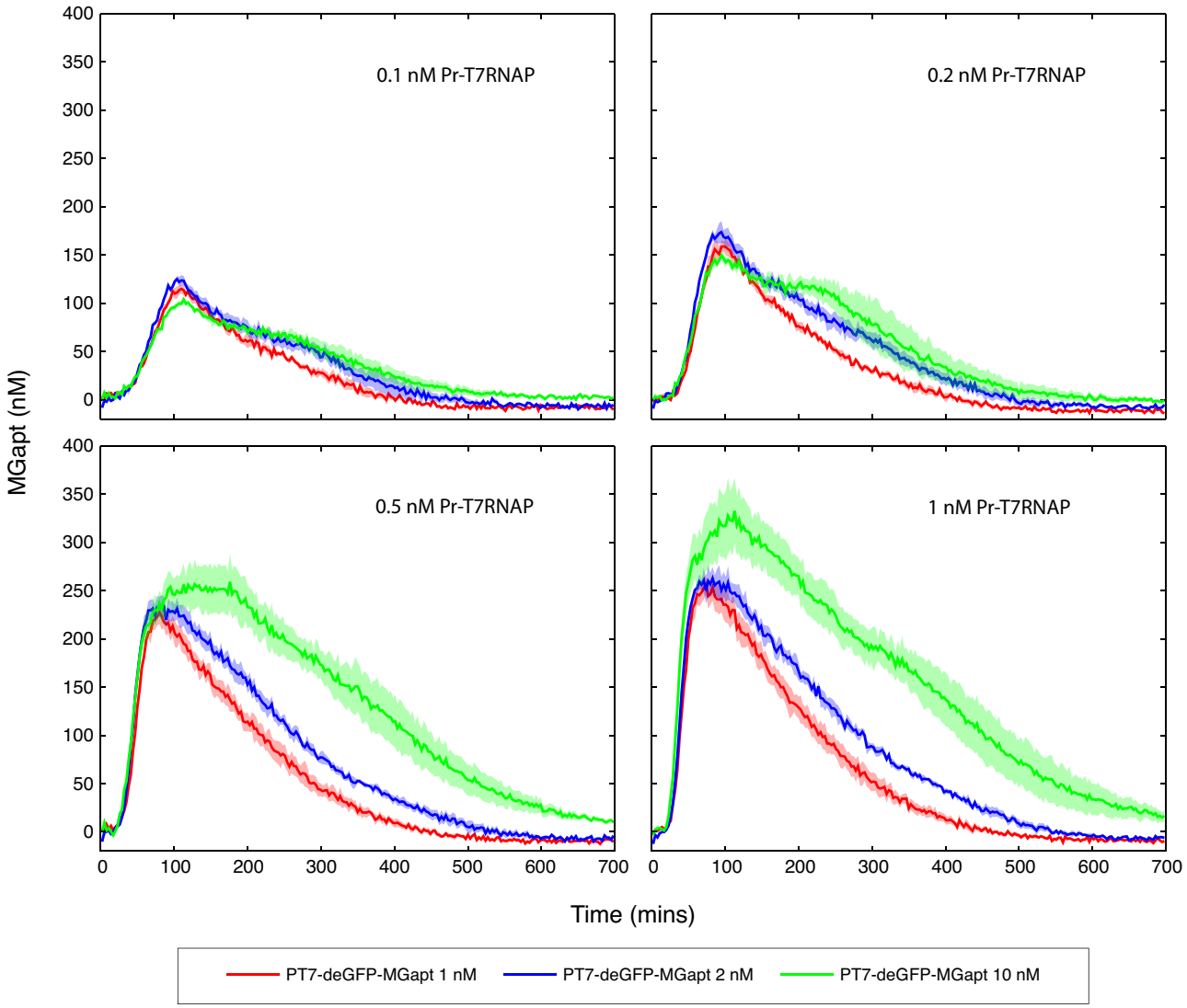

Figure S12: MGapt expression curves for T7 cascade tested with four different concentrations of first-stage T7 RNAP plasmid (0.1, 0.2, 0.5, and 1 nM Pr-T7 RNAP) and three different concentrations of the second-stage plasmid (1, 2, and 10 nM PT7-deGFP-MGapt). Shaded regions indicate standard error over replicates.

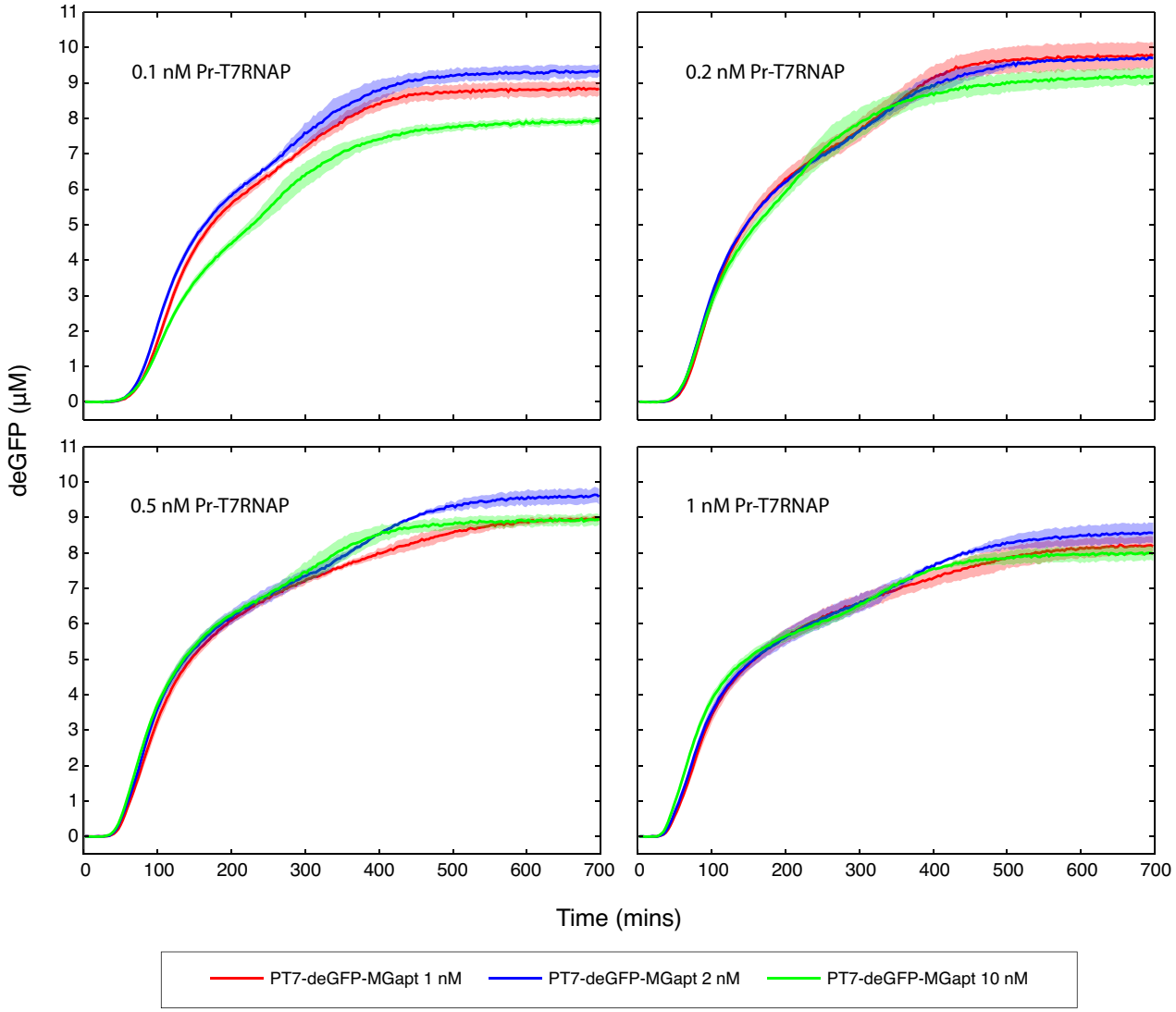

Figure S13: deGFP expression curves for T7 cascade tested with four different concentrations of the first-stage T7 RNAP plasmid (0.1, 0.2, 0.5, and 1 nM Pr-T7 RNAP) and three different concentrations of the second-stage plasmid (1, 2, and 10 nM PT7-deGFP-MGapt). Shaded regions indicate standard error over replicates.

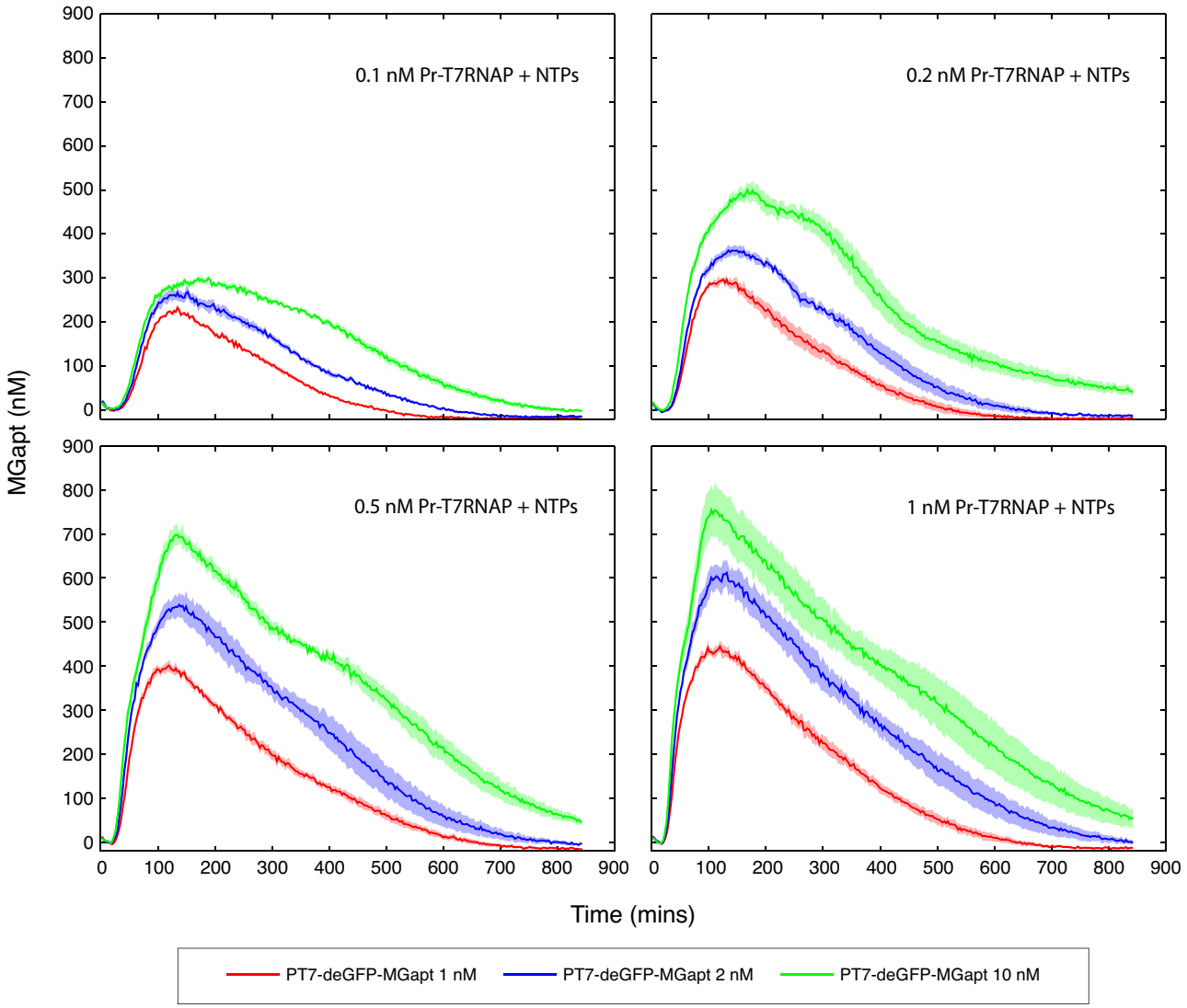

Figure S14: MGapt expression curves for T7 cascade tested with four different concentrations of first-stage T7 RNAP plasmid (0.1, 0.2, 0.5, and 1 nM Pr-T7 RNAP), three different concentrations of the second-stage plasmid (1, 2, and 10 nM PT7-deGFP-MGapt), and with the cell-free breadboard supplemented with 1.25 mM of each of the four NTPs. Shaded regions indicate standard error over replicates.

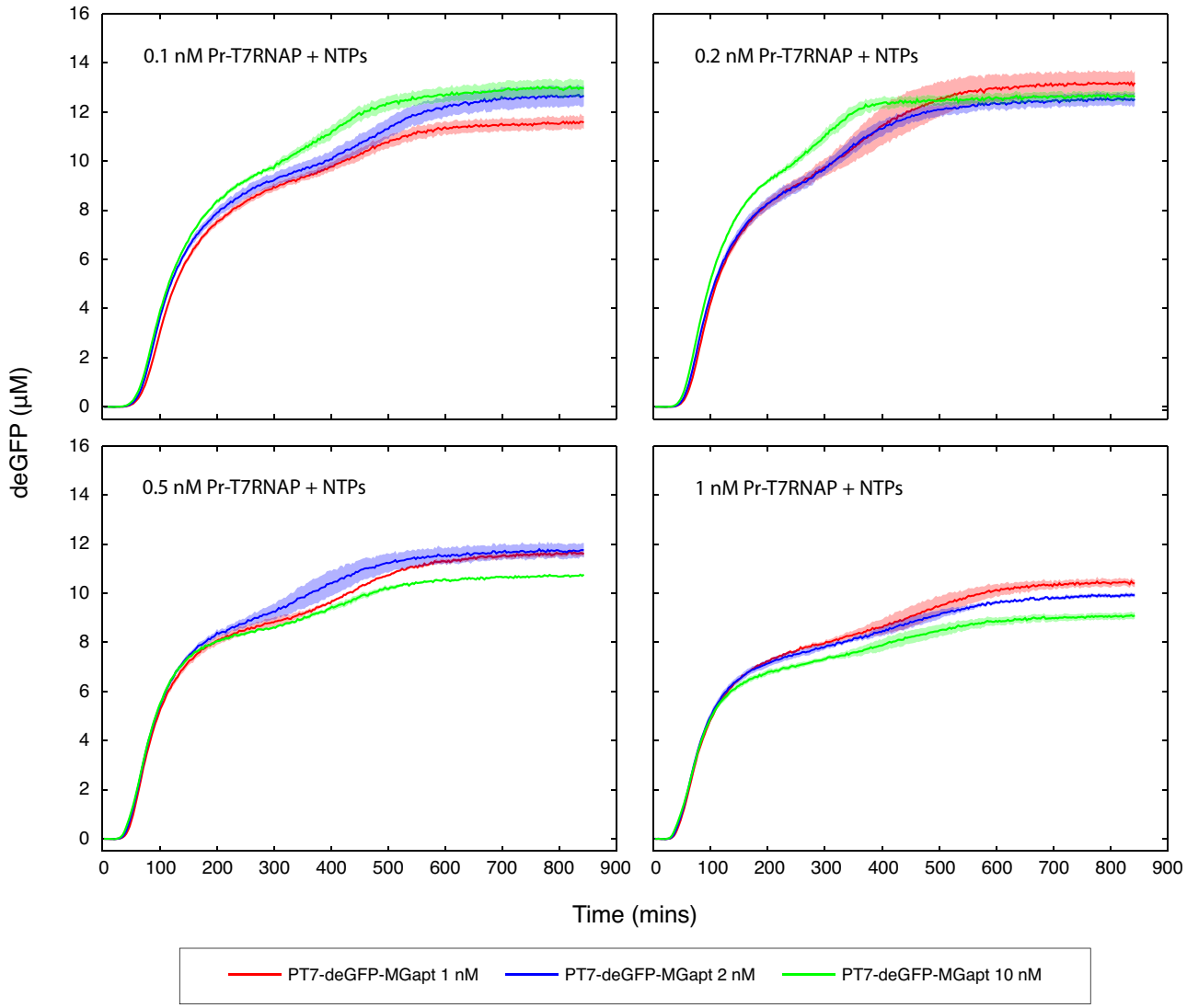

Figure S15: deGFP expression curves for T7 cascade tested with four different concentrations of the first-stage T7 RNAP plasmid (0.1, 0.2, 0.5, and 1 nM Pr-T7 RNAP), three different concentrations of the second-stage plasmid (1, 2, and 10 nM PT7-deGFP-MGapt), and with the cell-free breadboard supplemented with 1.25 mM of each of the four NTPs. Shaded regions indicate standard error over replicates.

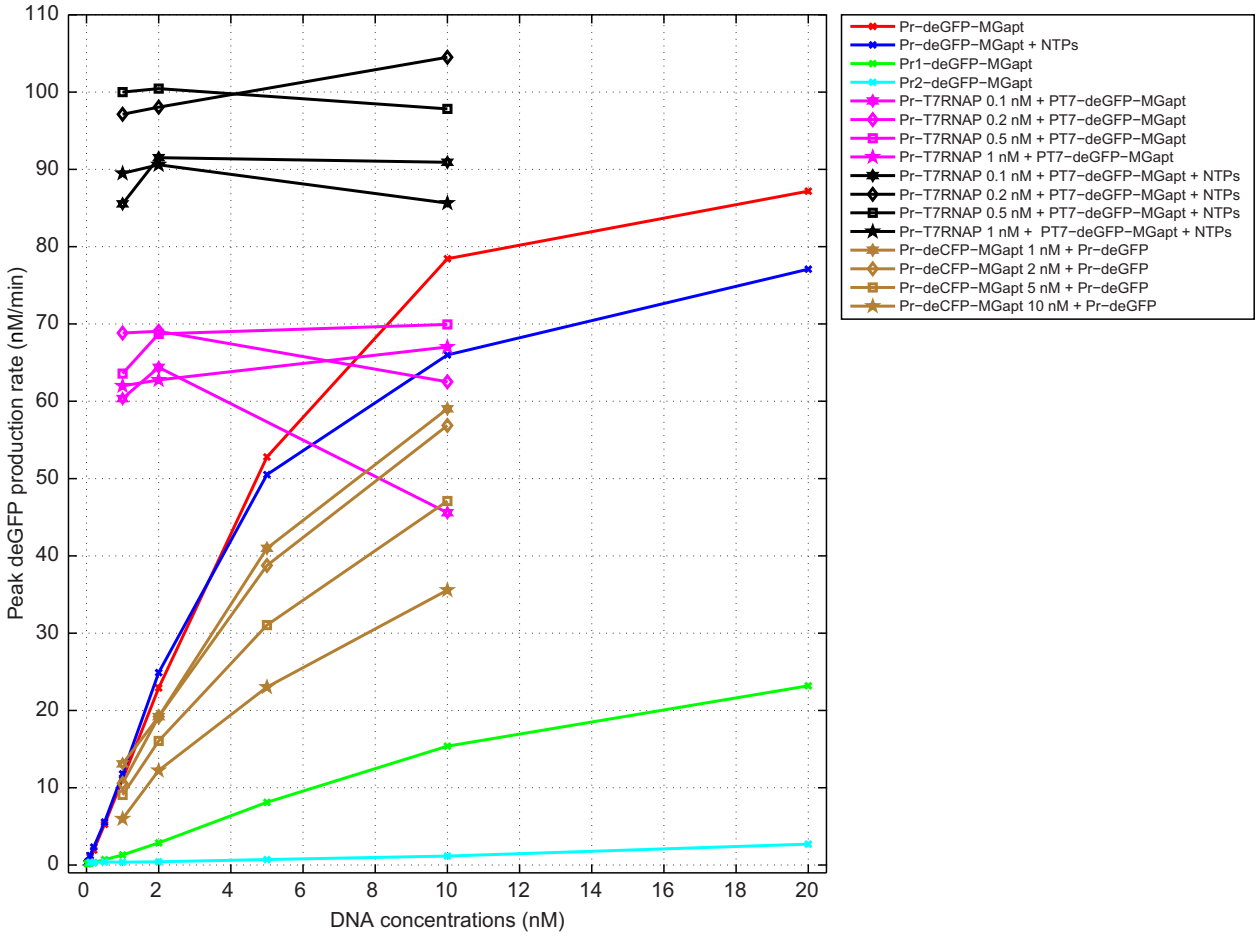

Figure S16: Maximum deGFP production rate as a function of reporter concentration under different conditions.

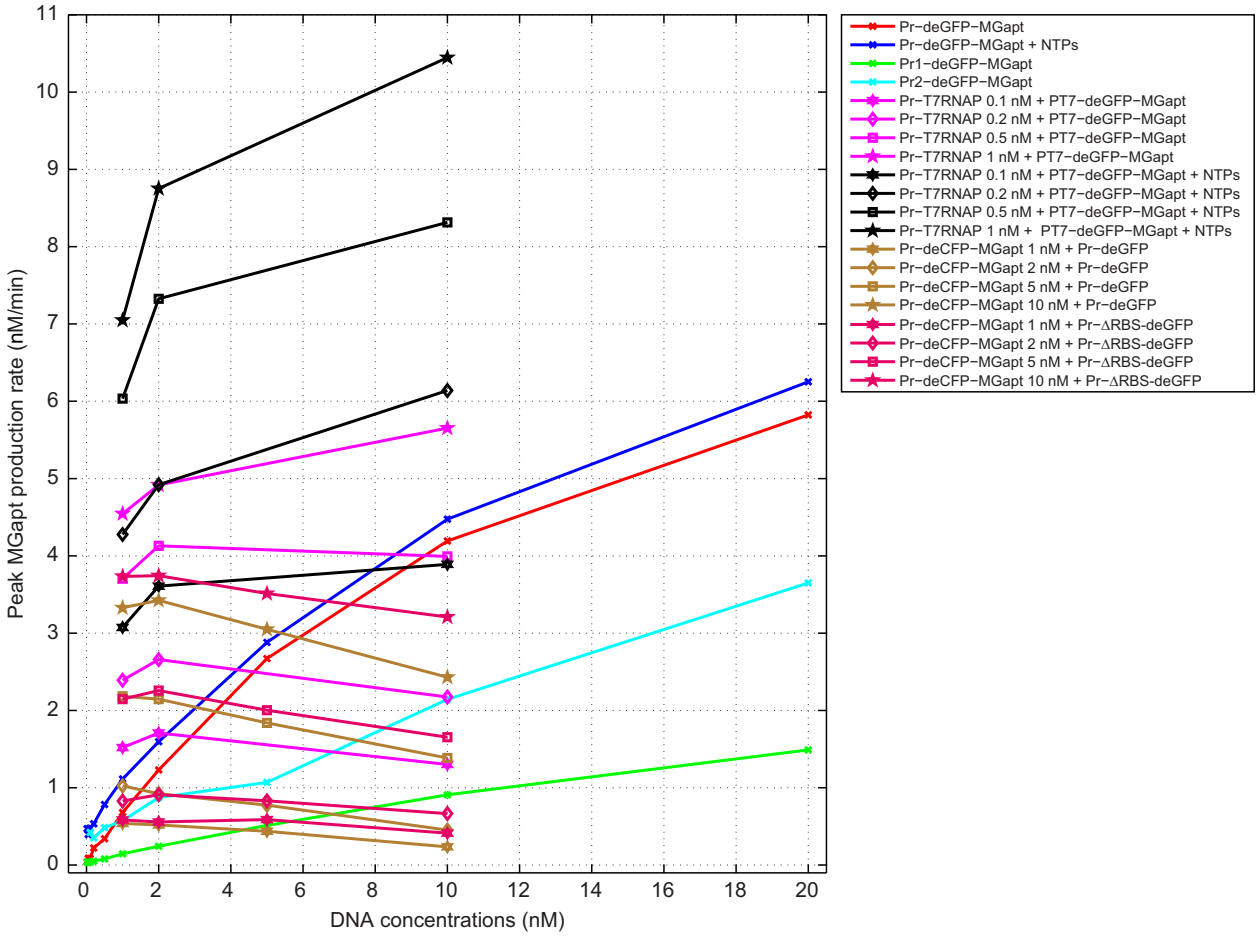

Figure S17: Maximum MGapt production rate as a function of reporter concentration under different conditions.

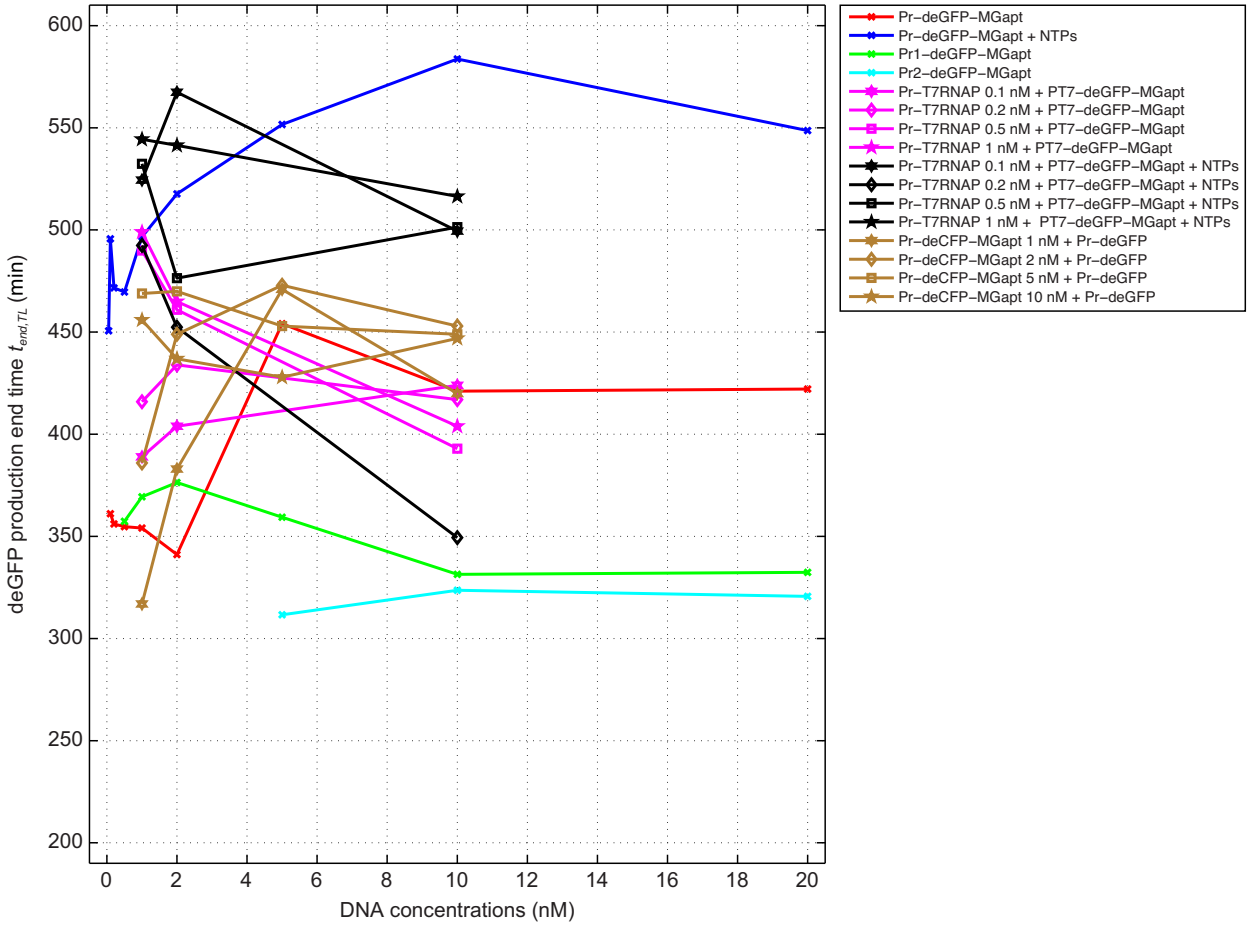

Figure S18: deGFP production end time $t_{end,TL}$ under different conditions.

Supplementary tables

Table S1: Genotypes of the plasmids used in this study.

Plasmid name	Transcription unit (TU)	TU size (bp)	Backbone/resistance
pBEST-Pr-GFP	P_R:deGFP:T500	810	ColE1/Amp^R
pBEST-Pr-ΔRBS-GFP	P_R:ΔRBS-deGFP:T500	775	ColE1/Amp^R
pBEST-Pr-GFP-MG	P_R:deGFP-MGapt:T500	869	ColE1/Amp^R
pBEST-Pr1-GFP-MG	P_{R1}:deGFP-MGapt:T500	869	ColE1/Amp^R
pBEST-Pr2-GFP-MG	P_{R2}:deGFP-MGapt:T500	869	ColE1/Amp^R
pBEST-Pr-CFP-MG	P_R:deCFP-MGapt:T500	869	ColE1/Amp^R
pBEST-Pr-T7RNAP	P_R:T7 RNAP:T500	3032	ColE1/Amp^R
pBEST-Pr1-T7RNAP	P_{R1}:T7 RNAP:T500	3032	ColE1/Amp^R
pBEST-Pr2-T7RNAP	P_{R2}:T7 RNAP:T500	3032	ColE1/Amp^R
pIVEX-pT7-GFP-MG	P_{T7}:deGFP-MGapt:T7term	939	ColE1/Amp^R